

Research report

Relative sparing of primary auditory cortex in Williams Syndrome

Dorothy P. Holinger^{a,b,c,*}, Ursula Bellugi^d, Debra L. Mills^{d,e}, Julie R. Korenberg^{f,g},
Allan L. Reiss^h, Gordon F. Shermanⁱ, Albert M. Galaburda^{a,b}

^aDivision of Behavioral Neurology, Beth Israel Deaconess Medical Center and Harvard Medical School, Boston, MA 02215, USA

^bDepartment of Neurology, Beth Israel Deaconess Medical Center and Harvard Medical School, Boston, MA 02215, USA

^cDepartment of Psychiatry, Beth Israel Deaconess Medical Center and Harvard Medical School, Boston, MA 02215, USA

^dLaboratory for Cognitive Neuroscience, The Salk Institute for Biological Studies, La Jolla, CA 92037, USA

^eDepartment of Psychology, Emory University, Atlanta, GA 30322, USA

^fCedars-Sinai Medical Center, Los Angeles, CA 90048, USA

^gDepartment of Pediatrics and Human Genetics, UCLA, Los Angeles, CA 90048, USA

^hNeuroimaging Laboratory, Department of Psychiatry and Behavioral Sciences, Stanford University School of Medicine, Stanford, CA 94305, USA

ⁱThe Newgrange School of Princeton, Princeton, NJ 08540, USA

Accepted 19 November 2004

Abstract

Williams Syndrome (WS) is a neurodevelopment disorder associated with a hemizygous deletion on chromosome 7. WS is characterized with mental retardation, severe visual–spatial deficits, relative language preservation, and excellent facial recognition. Distinctive auditory features include musical ability, heightened sound sensitivity, and specific patterns of auditory evoked potentials. These features have led to the hypothesis that the dorsal forebrain is more affected than the ventral. Previously, we reported primary visual area 17 abnormalities in rostral striate cortex, a region contributing to the dorsal visual pathway. Based on the dorsal–ventral hypothesis, and language and auditory findings, we predicted a more normal histometric picture in auditory area 41. We used an optical dissector method to measure neurons in layers II–VI of area 41 in right and left hemispheres of the same 3 WS and 3 control brains used in the area 17 study. There was a hemisphere by diagnosis interaction in cell packing density (CPD) in layer IV and in cell size in layer III between WS and control brains. Post hoc analysis disclosed in control brains, but not WS, a layer IV left > right asymmetry in CPD, and a layer III left < right asymmetry in cell size. WS brains showed more large neurons bilaterally in layer II and in left layer VI. Histometric alterations in area 41 were less widespread than rostral visual cortex. Also, there was less asymmetry in the WS brain. We interpret layers II and VI differences as reflecting increased limbic connectivity in primary auditory cortex of WS.

© 2004 Elsevier B.V. All rights reserved.

Theme: Sensory systems

Topic: Auditory systems: central anatomy

Keywords: Williams Syndrome; Primary auditory cortex; Area 41; Histometrics; Architectonics; Postmortem; Neuronal; Cell measures

1. Introduction

Williams Syndrome (WS) is a rare developmental disorder resulting in mild to moderate mental retardation and is characterized by distinctive brain, somatic, and cognitive features. WS is genetically defined by a hemizygous deletion of more than 20 contiguous genes on chromosome 7 q11.23, including the gene for elastin [23,25,35,36]. About 1 in 20,000 births demonstrate the deletion and accompanying

* Corresponding author. Division of Behavioral Neurology, Department of Neurology and Psychiatry, Beth Israel Deaconess Medical Center and Harvard Medical School, 330 Brookline Avenue, Boston, MA 02215, USA. Fax: +1 617 667 5217.

E-mail address: dholinge@bidmc.harvard.edu (D.P. Holinger).

phenotype [25,35,36,50]. There are, however, individuals with partial deletions who show partial phenotypic expression of WS [5,22,24]. WS individuals typically show severe visual–spatial impairment, marked by a preferential but fractionated attention to detail, and other mild-moderate cognitive deficits. Juxtaposed with these deficits, language function is relatively preserved and face recognition is excellent. This unique pattern of cognitive involvement has led to the hypothesis that there is a biased effect of the pathology on the dorsal visual pathways [1–3,16,17]. Visual–spatial functions are attributed to dorsal forebrain activity [1–3,46–48], whereas language and many auditory functions are typically associated with infrasyllian, therefore ventral localization [6,11,12,19,34,39,45]. With respect to auditory behaviors, WS individuals demonstrate an unusual profile, often showing hyperacusis [26,27,29,32] and auditory allodynia (displeasure toward certain sounds) [28]. They are also attracted to music and a variety of broadband noises [26,27]. The distinctive auditory sensitivity together with the cognitive strengths, weaknesses, and aberrations predict a relatively normal anatomy of the ventral cortices, including the primary auditory cortex [16].

The present histometric study of postmortem WS brains is part of a multidisciplinary project to describe and link cognitive, neuroimaging, neurophysiologic, anatomical, and genetic findings in WS. The anatomical studies in this laboratory, performed on autopsied specimens, have focused on cytoarchitectonic, histometric, and histochemical descriptions [15–18].

Given the dorsal–ventral hypothesis in WS, one focus of the microanatomic research in this laboratory has been to compare the histometric features between the dorsal and the ventral regions of the cerebral cortex. Our previous study of primary visual cortex showed histometric abnormalities affecting cortex underlying peripheral visual fields; these abnormalities were predicted because of the latter's special relationship to the dorsal visual pathway. They consisted of smaller neurons in 5 out of 8 layers in the left hemisphere [17]. In the present study of primary auditory cortex, we predicted it would be more normal than the rostral part of area 17 and would be congruent with findings made by our collaborators at different levels, e.g., a bilateral increase in electrophysiological responses (P200) to auditory stimuli [4,30] and an enlarged Heschl's [21] and superior temporal gyri (STG) [40]. In addition, Levitin and colleagues [27] reported a bilateral increase in fMRI activation to musical stimuli in the STG, middle temporal gyrus, and superior temporal sulcus in WS.

2. Materials and methods

2.1. Subjects

We examined primary auditory cortex in age- and sex-matched autopsy specimens from 3 WS subjects (1 male and

2 females) and 3 control subjects (1 male and 2 females). These brains were the same as those reported in a previous study [17]. The WS cases were diagnosed in life on the basis of somatic characteristics and the results of fluorescent in situ hybridization (FISH) for the missing elastin gene. The control cases were free from neurological problems, and, after examination of medical records, proved negative for psychiatric or medical illness (the Harvard Brain Tissue Resource Center, HBTRC, McLean Hospital, Belmont, MA). There was no information on handedness.

2.2. Histology

One WS brain (Subject 1) was processed using the Yakovlev [52] whole-brain method of serial histological sections. In this method, after fixing the brain in 10% formalin, it is dehydrated in a series of graded alcohols and embedded in 3%, 6%, and 12% celloidin. Afterwards, the brain is sectioned coronally at 35 μ m, and every 20th section is stained with Cresylechtviolett for Nissl substance. The postmortem brain tissue from the remaining WS and all control brains was processed in the following histological manner. Small blocks of tissue (2 \times 2 \times 2 cm) were dissected from mid-Heschl's gyrus in the left and right hemispheres and stored in 10% formalin until they were dehydrated in a series of graded alcohols. The blocks were then embedded in 3%, 6%, and 12% celloidin, sectioned at 30 μ m, and every 10th section was stained with Cresylechtviolett for Nissl substance.

2.3. Area 41 cytoarchitecture

Following Brodmann's [7] cytoarchitectonic definition of area 41 as primary auditory cortex, subsequent studies have shown several cytoarchitectonic subdivisions and considerable variability with regard to its borders [14,31,37,38,49]. We sampled from medial auditory koniocortex (KAm) in area 41, the main efferent target of the medial geniculate nucleus located on the medial half of Heschl's gyrus in coronal sections. KAm is characterized by its highly granular or sandy appearance [14,31] and is exceedingly extemodense. That is, KAm has greater cell packing density in layers II, III, and IV than in layers V and VI. Layer IV is not subdivided as in visual area 17, and is very broad and deeply invades into overlying layer III, thus blurring the border between the two layers. KAm is easily identified in stained sections even with the naked eye, and in myelin stained preparations is by far the most myelinated region in the temporal lobe.

2.4. Cell counting and measuring procedures

Area 41 Nissl-stained sections in the WS and control brains were identified based on the cytoarchitecture described above. Three fields from the pial surface to the grey–white matter junction were chosen where the plane of

section was perpendicular or near perpendicular to the pial surface of Heschl's gyrus, and there was no distortion by rippling, tears or other artifacts. With regard to plane of section, we make every effort to orient the plane of section to be perpendicular to the pial surface. Whatever deviation from this plane unwittingly is likely to affect the WS and the control brains equally. We don't have a hypothesis that within the cortex the WS and control neurons adopt different orientations, which obviates the need to correct for that possibility. We are not concerned with absolute measurements but with measurements in one group relative to the other. Therefore, we believe the methods are as unbiased as possible. Finally, given the well-known effects on cortical layers and the cells comprising them with regard to curvature around sulci and gyri, we also make special efforts in order to compare cases that are equivalently placed with respect to gyri and sulci.

All sections were coded so that the examiner was blind to diagnosis and hemisphere. The architectonic appearance of area 41 in WS (Fig. 1) is on the whole indistinguishable from that in the controls (Fig. 2) so this form of blinding was deemed to be adequate. Neurons were identified by the presence of a clearly visible, single large nucleolus, a feature that distinguishes them from glial cells, which often exhibit a speckled pattern of nuclear chromatin. (Glial cells also have a smaller rim of cytoplasm and a thicker cell membrane [44]).

The modified dissector method software of Williams and Rakic [51] was used to measure neurons in layers II, III, IV, V, and VI in the right and left hemispheres. This method creates an exactly reproducible 3-dimensional count box that does not include the upper and lower surfaces of the section thus eliminating the need to have sections of the same thickness or perfectly regular sections. Using a Zeiss Universal microscope under $\times 500$ oil magnification, images captured by a Vidicon camera were displayed on

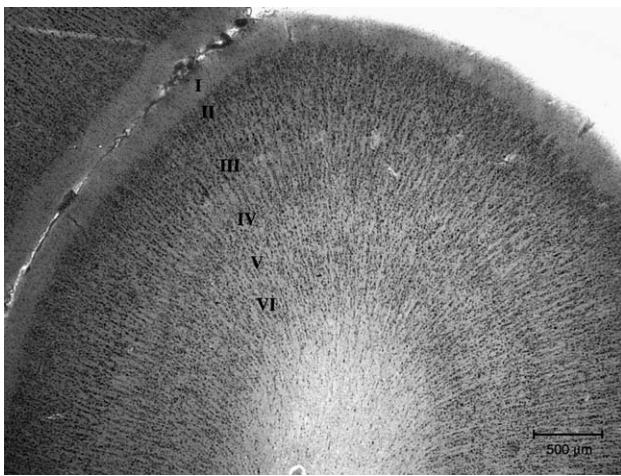


Fig. 1. This photomicrograph depicts the cytoarchitectonic characterization of area 41 in a Nissl-stained section in a WS brain. Area 41 is characterized by its highly granular appearance and greater neuronal density in layers II, III, and IV than in layers V and VI.

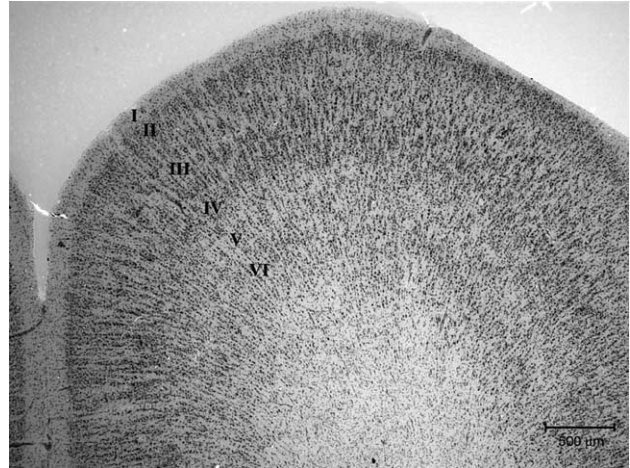


Fig. 2. This photomicrograph depicts the cytoarchitectonic characterization of area 41 in a Nissl-stained section in a control brain.

a Sony GVM 1310 monitor that was connected to a Macintosh Centris 650 workstation. The 3-dimensional count box ($95 \mu\text{m} \times 85 \mu\text{m} \times 20 \mu\text{m}$) was placed within these images. A Heidenhain MP-25 photoelectric micrometer interfaced to a National Instrument NB-GPIB card in the Macintosh recorded movement in the z-axis. The base of the sections was set to a z-axis reading of zero. A red opaque overlay precluded cell counting below the dimensions of the counting box. With the movement of the stage to $5 \mu\text{m}$ (7.5 for Subject 1) above the original position of the base of the section, the screen became transparent and the cells visible. The soma of the neurons was traced on a digitizing tablet, whereby neurons touching the top and left side of the screen were excluded. At a stage level of more than $25 \mu\text{m}$ (27.5 for Subject 1) above the original position of the base of the section, the screen turned opaquely green, preventing measurement of cells above the counting box.

Cell packing density was defined as the number of neurons per unit volume (μm^3) and was estimated with the use of a 3-dimensional count box ($95 \mu\text{m} \times 85 \mu\text{m} \times 20 \mu\text{m}$), a method [51] used in previous studies [17,44] and described above. Three fields containing area 41 were chosen for cell density measurements. Count boxes were generated for each of the 3 fields and all identified neurons were counted within a stack of individual count boxes. Specifically, individual count boxes were generated for each layer in each of the 3 fields to determine cell packing density for each case. After a layer was identified at low power ($5\times$), the experimenter would switch to a $40\times$ objective so that the density could be calculated within each of the 5 layers. Values from the count boxes in all 3 designated fields were averaged to determine cell density for each case for every layer in each hemisphere.

Cell size was also measured with the count box method along with a digitizing tablet on which outlines of neuronal soma were traced with a stylus. Cross-sectional neuronal

areas (μm^2) were derived from the calculation of a diameter of a circle with equal area for each of these measurements. Average diameters for all cells were obtained for each layer for each brain in each hemisphere. The means for the WS brains and the control brains were calculated to obtain group means. In addition to determining mean neuronal size, we also examined the frequency distribution of cell size. Based on our previous studies [17], this method has proven to be a sensitive way to elucidate group differences.

2.5. Statistical analysis

Repeated-measures ANOVA was used to determine cell packing density and neuronal size differences between the WS and control brains. Diagnosis (WS and controls) was the between-subjects factor, and hemisphere and layer were the within-subjects factors. The effect of gender could not be analyzed with any confidence because of the small number of cases. Given the marked variability in neuronal size, as is the case in the cerebral cortex, demonstrating significant neuronal differences in the situation where large and small neurons increase in numbers can be difficult. For example, the neuronal area in one control brain (Table 1, brain #4) for each layer in the left hemisphere measured: layer II: $59.5 \mu\text{m}^2$; layer III: $104.8 \mu\text{m}^2$; layer IV: $63.1 \mu\text{m}^2$; layer V: $75.7 \mu\text{m}^2$; and layer VI: $92.8 \mu\text{m}^2$, whereas cell areas in this brain the right hemisphere measured: layer II: $89.7 \mu\text{m}^2$; layer III: $112.1 \mu\text{m}^2$; layer IV: $67.9 \mu\text{m}^2$; layer V: $116.9 \mu\text{m}^2$; and layer VI: $111.6 \mu\text{m}^2$. Therefore, to assess additional differences in neuronal size in each layer, the frequency distributions of cell size were analyzed using χ^2 tests.

3. Results

3.1. Brain data

These brains, which were used in a previous study [17], showed a significant decrease in brain weight (WS: 1033 ± 104 g; controls: 1426 ± 177 g) ($P < 0.05$). There were no significant differences ($P > 0.05$) between the two groups in PMI (WS: 25.5 ± 3.3 h; controls: 18.4 ± 6.1 h), TF (WS: 12.17 ± 1.84 months; controls:

14.9 ± 2.72 months), or in age (WS: 43.3 ± 11 years; controls: 44 ± 14 years).

3.2. Cell packing density (CPD)

Repeated-measures ANOVA revealed significant CPD effects between the WS and control brains. First, as predicted on the basis of known differences in neuronal types among layers, there was a significant effect of layer overall ($F = 98.79$, $df = 4,16$, $P < 0.0001$), and also for each the left ($F = 53.25$, $df = 1,4$, $P < 0.0001$) and right hemispheres ($F = 59.75$, $df = 1,4$, $P < 0.0001$). Separate analysis for layer IV revealed a hemisphere by diagnosis interaction ($F = 20.00$, $df = 1,4$, $P < 0.01$) (Fig. 1), which on further analysis revealed more highly packed neurons in the left hemisphere ($170,897$ neurons/ mm^3) than in the right ($156,656$ neurons/ mm^3) in the control brains ($F = 91.23$, $df = 1,4$, $P < 0.002$). The lack of significant asymmetry in the WS brains may be due to the increased variability in cell density (Fig. 3). There were no other significant group differences.

3.3. Neuronal size

Repeated-measures ANOVA analyses of cross-sectional mean neuronal areas also revealed, as expected, a main effect of layer overall ($F = 40.44$, $df = 1,4$, $P < 0.0001$) and for the left ($F = 26.83$, $df = 1,4$, $P < 0.0001$) and right hemispheres separately ($F = 20.95$, $df = 1,4$, $P < 0.0001$). A hemisphere by diagnosis interaction was significant in layer III ($F = 20.18$, $df = 1,4$, $P < 0.01$) (Fig. 2). Further analyses of layer III in the left hemisphere showed that, in the WS brains, there was a tendency ($P < 0.056$) toward larger neurons ($111 \mu\text{m}^2$) compared to the control brains ($96 \mu\text{m}^2$). The control brains, but not the WS brains, showed a left > right asymmetry, with smaller neurons in the left ($96 \mu\text{m}^2$) compared to the right ($104 \mu\text{m}^2$) hemisphere ($P < 0.04$). The lack of significant asymmetry in the WS brains may be due to the increased variability in neuronal size (Fig. 4).

3.4. Neuronal size distributions

To assess for additional differences in overall neuronal size and each layer separately, we analyzed the frequency

Table 1
Descriptive data of Williams and control brains

Brain	Race	Diagnosis ^a	Age	Sex	Postmortem interval (h)	Time in formalin (months)	Brain weight (g)	Cause of death
1	W	W	31	M	26.2	12.6	1150	Cardiac
2	W	W	53	F	22.0	14.2	950	Cardiac
3	W	W	46	F	28.5	13.7	1000	Cancer
4	W	C	58	F	21.5	18	1319	Cardiac
5	W	C	44	F	10.7	12.8	1329	Cardiac
6	W	C	30	M	23.0	14	1630	Cardiac

^a W = Williams Syndrome; C = Control.

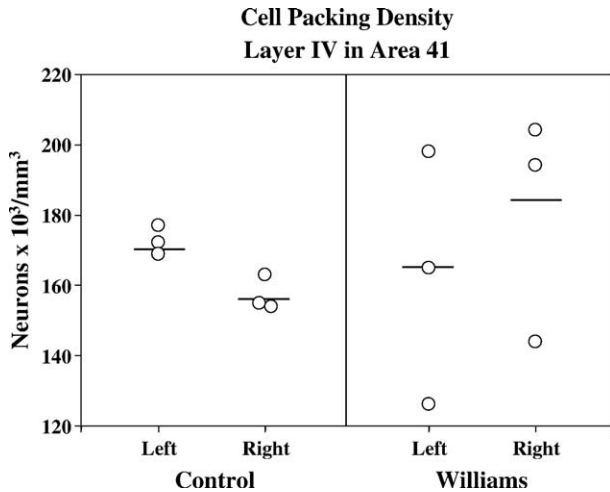


Fig. 3. Plots of individual case values for cell packing density are shown for layer IV in area 41. Cell density in the control brains in the left and right hemispheres is shown in the left plot, and in the WS brains in the right plot. There was a significant interaction between hemisphere and diagnosis ($F = 20.00$, $df = 1,4$, $P < 0.01$) in layer IV. There was a significant left > right asymmetry in the control brains ($P < 0.002$), but no significant asymmetry in the WS brains, a result that may be due to the large variability in this group.

distribution of cell sizes in consecutive bins arranged in ascending size order. The number of bins ranged between 8 and 11, increasing in stepwise fashion by 10 μm^2 , and contained neurons whose sizes ranged from 40 to 110 μm^2 . Chi-square values were calculated for the neuronal distribution in these bins between WS and control brains. We also examined asymmetry in the distribution of cell sizes, both in WS and controls. As in previous studies, we set α at 0.001 for rejection of the null hypothesis to compensate for the high sensitivity of this test [17].

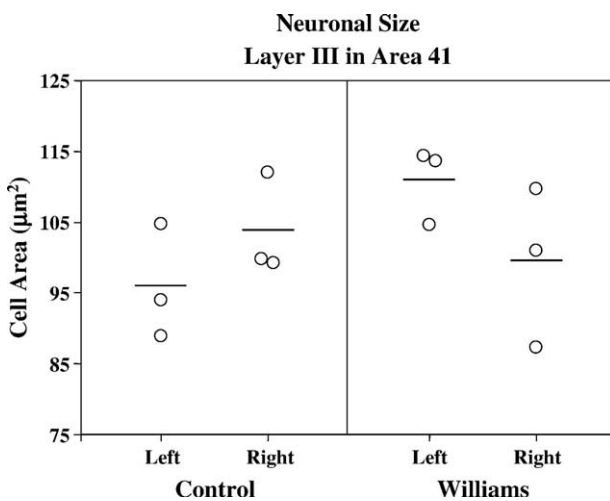


Fig. 4. Plots of individual case values for neuronal size are shown for layer III in area 41. Neuronal size in the control brains in the left and right hemispheres is shown in the left plot, and for the WS brains in the right plot. There was a significant interaction between hemisphere and diagnosis ($F = 20.18$, $df = 1,4$, $P < 0.01$) in layer III. The left < right asymmetry in the control brains was significant ($P < 0.04$). The lack of any significant asymmetry in the WS brains could be due to the large variability.

We examined each layer collapsed over both hemispheres between controls and WS. There were significant differences for layer II ($\chi^2 = 75.63$, $df = 8$, $P < 0.0001$) and layer VI ($\chi^2 = 47.57$, $df = 10$, $P < 0.0001$), whereas WS brains had an excess of large neurons compared to the control brains. Separate analyses of each hemisphere showed that the WS brains had an excess of large neurons in layer II in the left ($\chi^2 = 47.92$, $df = 10$, $P < 0.0001$) and right hemispheres ($\chi^2 = 41.15$, $df = 8$, $P < 0.0001$) (Figs. 5 and 6), and only in left layer VI ($\chi^2 = 37.00$, $df = 10$, $P < 0.0001$). There were no significant asymmetries in cell size distribution overall or layer-by-layer in either group. However, at $P < 0.05$, and consistent with the findings of mean cell area asymmetry in layer III in the control brains (see above), the cell distribution in this layer for the controls showed greater numbers of small neurons in the left side.

4. Discussion

The present study defined several anatomic features in WS brains. First, as in the previous study with the same brains [17], there was a demonstrable decrease in brain weight compared to control brains. The finding of a significantly smaller brain in WS may be accounted for predominantly by a reduction in the size of the posterior portions of the forebrain regions, including the occipital lobes [40]. Second, histometric findings associated with this gross posterior curtailment include an increase in visual cortical cell packing density and excess of small neurons in

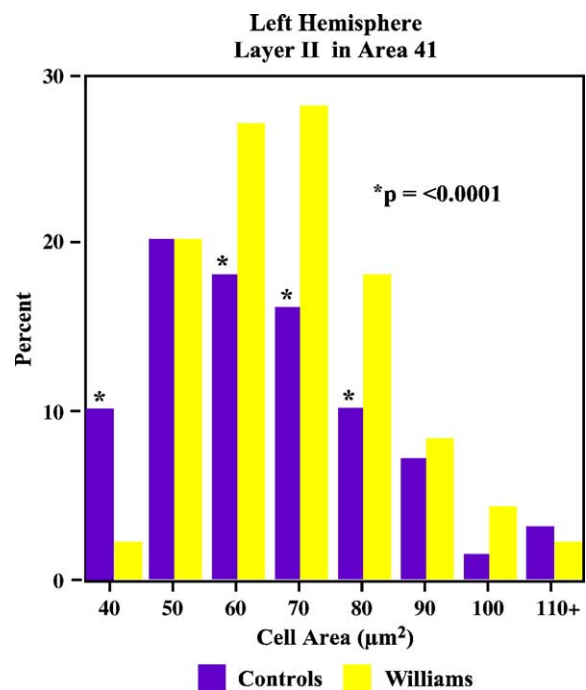


Fig. 5. Layer II of the left hemisphere: There was a significant difference between WS and controls ($\chi^2 = 33.67$, $df = 8$, $P \leq 0.0001$) with more large cells and fewer small cells in the WS brains compared to the control brains.

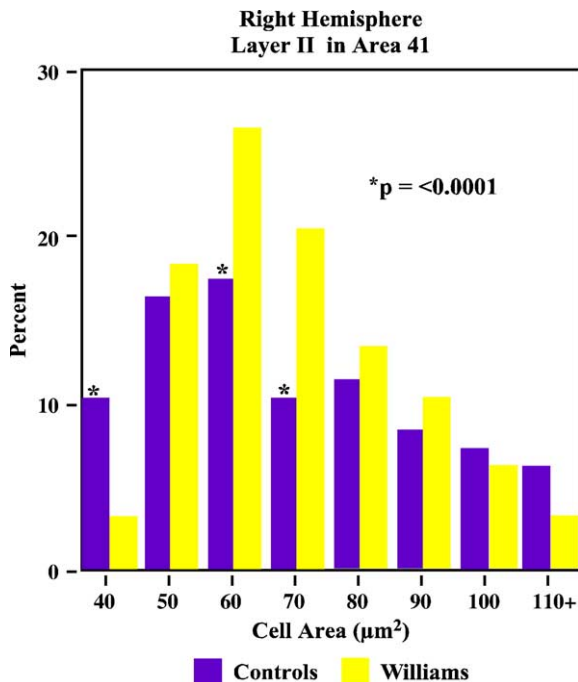


Fig. 6. Layer II of the right hemisphere: There was a significant difference between WS and controls ($\chi^2 = 41.15$, $df = 10$, $P < 0.0001$) with more large cells and fewer small cells in the WS brains compared to the control brains.

some of the layers projecting to the dorsal visual pathway [17]. On the other hand, the superior temporal brain regions are not grossly curtailed and may even be increased in size [21,40]. In the present histometric study, we found no significant differences in cell packing densities and cell sizes between WS and control brains in the primary auditory cortex, other than in the degree of brain asymmetry in some of these measures. However, WS brains showed an excess of larger neurons in layer II bilaterally and in layer VI on the left side compared to control brains.

Whereas asymmetries in neuronal packing density could be demonstrated in control brains, WS brains showed no such asymmetries. Further, an asymmetry in neuronal size in layer III was demonstrated in control brains but not in WS brains. This finding in the control brains agrees with Morosan et al. [31] and Rademacher et al. [37] who reported a left > right asymmetry in area 41 using a grey level index (GLI) [31] and planimetry [37]. Although other measures can be confounded by large differences in cell size within the same range of cell density, the variability in the cortex in cell sizes is such that there's probably a good correlation between our measure of cell density and their measures. Curiously, therefore, in standard lateralization, smaller more densely packed neurons may be part of the anatomical substrate of language in the left hemisphere, even though such a finding is counterintuitive. By contrast, that the WS brains did not show asymmetry may reflect an unusual organization for language lateralization, a statement that could be tested experimentally using functional brain imaging. On the other hand, the amount of variability in the

WS asymmetry data could have obscured a finding of asymmetry. While not much is known about functional lateralization in WS (but see [30]), this information could be readily obtained in future studies. Regarding the possible causes of the altered asymmetry in WS, it may reflect a specific genetic effect related to the deletion; it may also result from a nonspecific effect of anomalous development [20], whereas less right-handedness or less cerebral asymmetry of the standard pattern is a common result of interference with normal brain development [42].

There were no significant differences in cell packing densities or cell sizes in the auditory cortex of WS compared to the control brains. Given the larger variability of measurement in the WS group, or issues relating to sample size, real differences may not have been detectable in this study. Yet, a trend for larger neurons in layer III ($P < 0.056$) was seen. The absence of significant group differences in area 41 contrasts with the demonstrable differences in cell packing differences and cell sizes seen in rostral area 17 in the same series of brains. One interpretation is that the primary auditory cortex of WS subjects is more normal than the rostral primary visual cortex, a conclusion supporting the finding of a more abnormal dorsal visual cognitive profile than auditory function.

One could further hypothesize that the greater proportion of larger neurons in auditory layer II in WS brains is related to unusual auditory function. In monkeys, it has been shown that cortical input into adjacent cortical visual and auditory areas differs according to whether the input is coming from rostral or from caudal sources. Thus, a given cortical area receives projections from more caudally located neighbors directed to layer IV, while projections from their more rostrally located neighbors arrive in layer II [13,41]. In the case of the auditory cortices, temporopolar areas with limbic connectivity to the amygdala project to layer II of more caudally located auditory cortical areas. We might therefore interpret the enlarged layer II neurons in area 41 in WS as indicating that the auditory cortex is more limbically connected than in the normal state, and perhaps this is the reason for enhanced sensitivity and emotionality to sound in this population. For instance, WS subjects show a strong aversion to high-frequency sounds, becoming quite fearful and distressed, and also often demonstrate an unusual attraction to other sounds, including music [26–29,32]. Regarding the findings in left layer VI, it is difficult to know how they relate to the WS phenotype, although most neurons in this layer participate in the function of the cortico-thalamic loop and are in a position to change the response properties of thalamic auditory neurons [8].

Structural imaging studies have shown an enlarged superior temporal gyrus and Heschl's gyrus in WS brains [21,40]. In addition, Schneider and colleagues [43] showed that increased tissue volume (structural MRI) and greater MEG activation in Heschl's gyrus were significantly correlated, suggesting that, indeed, anatomical size can determine signal strength in the auditory cortex. The

histometric findings presented here cannot explain the gross anatomical difference in the temporal lobe, as it is unlikely that a slight over-proportion of larger neurons in layer II and/or VI can account for larger superior temporal and Heschl gyri. However, there may be a larger number of neurons in absolute terms, either because of enlarged territories occupied by auditory cortex, or deeper cortical columns containing more, albeit highly packed, neurons. The present study does not address these possibilities, but we are aware that the extent of architectonic areas can vary greatly [14,31,37,38,49,53] and that claims have been made regarding variability in the lengths of cortical columns as part of normal diversity and in relationship to developmental abnormalities [9,10,33].

In summary, there are both gross anatomical and histometric changes that characterize the WS brain. The WS brain is smaller and the major telencephalic curtailment is seen in the posterior portions of the hemispheres. Supporting this gross anatomical finding is the finding of abnormal visual–spatial function in WS as well more highly packed, smaller neurons in some of the layers of the primary visual cortex subserving the dorsal visual system. By contrast, the gross anatomy of auditory regions is not reduced, but instead is increased in size and no significant histometric changes, other than an excess of some pyramidal neurons, are found following histometric analysis. Furthermore, because so few layers were affected, and those that were, showed more large neurons, the primary auditory cortex looks more normal by histometric criteria. Of additional interest is the possibility that an excess of larger layer II pyramidal cells in area 41 of WS brains may reflect hyperconnectivity to the limbic system, which may in turn help explain the unusual sensitivity to sounds exhibited by WS individuals. Finally, this and previous studies seem to suggest altered cerebral asymmetry in WS, thus suggesting additional research on functional cerebral lateralization in these subjects.

Acknowledgments

The research presented in this manuscript was supported by an NIH grant HD33113 to UB at the Salk Institute. We are grateful to the families who have donated the Williams and control brains and to the local, regional, and national Williams Syndrome Associations. The brain tissue for controls was provided by the Harvard Brain Tissue Resource Center supported in part by PHS MN/NS 31862. We thank Antis Zalkalns for his technical support. Dan McMenamin carried out part of the measurements.

References

- [1] J. Atkinson, J. King, O. Braddick, L. Nokes, S. Anker, F. Braddick, A specific deficit of dorsal stream function in Williams' syndrome, *NeuroReport* 8 (1997) 1919–1922.
- [2] J. Atkinson, S. Anker, O. Braddick, L. Nokes, A. Mason, F. Braddick, Visual and visuospatial development in young children with Williams syndrome, *Dev. Med. Child Neurol.* 43 (2001) 330–337.
- [3] J. Atkinson, O. Braddick, S. Anker, W. Curran, J. Wattam-Bell, F. Braddick, Neurobiological models of visuospatial cognition in children with Williams syndrome: measures of dorsal-stream and frontal function, *Dev. Neuropsychol.* 23 (1–2) (2003) 139–172.
- [4] U. Bellugi, D.L. Mills, T. Jernigan, G. Hickok, A.M. Galaburda, Linking cognition, brain structure and brain function in Williams Syndrome, in: H. Tager-Flusberg (Ed.), *Neurodevelopmental Disorders: Contributions to a New Framework from the Cognitive Neuroscience*, MIT Press, Cambridge, MA, 1999, pp. 111–136.
- [5] U. Bellugi, L. Lichtenberger, D. Mills, A. Galaburda, J.R. Korenberg, Bridging cognition, the brain and molecular genetics: evidence from Williams syndrome, *Trends Neurosci.* 5 (1999) 197–207.
- [6] I. Biederman, P.C. Gerhardstein, E.E. Cooper, C.A. Nelson, High level object recognition without an anterior inferior temporal lobe, *Neuropsychologia* 35 (1997) 271–287.
- [7] K. Brodmann, Vergleichende lokalisationslehre der grosshirnrinde in ihren prinzipien dargestellt auf grund des zellenbaues, JA Barth, Leipzig, 1909.
- [8] J.C. Brumberg, F. Hamzei-Sichani, R. Yuste, Morphological and physiological characterization of layer VI corticofugal neurons of mouse primary visual cortex, *J. Neurophysiol.* 89 (5) (2003) 2854–2867.
- [9] D.P. Buxhoeveden, M.F. Casanova, The minicolumn hypothesis in neuroscience, *Brain* 125 (2002) 935–951.
- [10] M.F. Casanova, D.P. Buxhoeveden, A.E. Switala, E. Roy, Neuronal density and architecture (Gray Level Index) in the brains of autistic patients, *J. Child Neurol.* 17 (7) (2002) 515–521.
- [11] A.R. Damasio, N. Geschwind, The neural basis of language, *Annu. Rev. Neurosci.* 7 (1984) 127–147.
- [12] J.A. Fiez, M.E. Raichle, Linguistic processing, *Int. Rev. Neurobiol.* 41 (1997) 233–254.
- [13] A.M. Galaburda, D.N. Pandya, The intrinsic architectonic and connective organization of the superior temporal region of the macaque, *J. Comp. Neurol.* 221 (1983) 169–184.
- [14] A. Galaburda, F. Sanides, Cytoarchitectonic organization of the human auditory cortex, *J. Comp. Neurol.* 190 (1980) 597–610.
- [15] A.M. Galaburda, U. Bellugi, Multi-level analysis of cortical neuroanatomy in Williams syndrome, *J. Cogn. Neurosci.* 12 (2000) 74–88.
- [16] A.M. Galaburda, P.P. Wang, U. Bellugi, M. Rossen, Cytoarchitectonic anomalies in a genetically based disorder: Williams syndrome, *NeuroReport* (1994) 758–787.
- [17] A.M. Galaburda, D.P. Holinger, U. Bellugi, G.F. Sherman, Williams Syndrome: neuronal size and neuronal-packing density, *Arch. Neurol.* 59 (2002) 1461–1467.
- [18] A.M. Galaburda, D.P. Holinger, U. Bellugi, J.R. Korenberg, P. Itoka, GTF2I Immunostaining in area 17 in Williams Syndrome, Society for Neuroscience annual meeting, Orlando, FL, Neurosci. Abstr. (2002).
- [19] I. Gauthier, M.J. Tarr, J. Moylan, P. Skudlarski, J.C. Gore, A.W. Anderson, The fusiform “face area” is part of a network that processes faces at the individual level, *J. Cogn. Neurosci.* 12 (2000) 495–504.
- [20] N. Geschwind, A.M. Galaburda, *Cerebral lateralization: biological mechanisms, associations and pathology*, MIT Press, Cambridge, 1987.
- [21] G. Hickok, U. Bellugi, W. Jones, Asymmetrical ability, *Lett. Sci.* 270 (5234) (1995) 219–220.
- [22] H. Hirota, R. Matsuoka, X.-N. Chen, L.S. Salandanan, A. Lincoln, F.E. Rose, M. Sunahara, M. Osawa, U. Bellugi, J.R. Korenberg, Williams syndrome deficits in visual spatial processing linked to GTF2IRD1 and GTF2I on Chromosome 7q11.23, *Genet. Med.* 5 (4) (2003) 311–321.
- [23] J.R. Korenberg, X.-N. Chen, D. Yimlamia, R. Bisighini, U. Bellugi, Williams syndrome: the search for the genetic origins of cognition, *Am. J. Hum. Genet* (abstract) 61 (4) (1997) A103.

- [24] J.R. Korenberg, X.-N. Chen, H. Hirota, Z. Lai, U. Bellugi, D. Burian, B. Roe, R. Matsuoka, Genome structure and cognitive map of Williams syndrome, *J. Cogn. Neurosci.* 12 (2000) 89–107.
- [25] J.R. Korenberg, U. Bellugi, L.S. Salandanan, D.L. Mills, A.L. Reiss, A neurogenetic model of human behavior, in: D.N. Cooper (Ed.), *Encyclopedia of the Human Genome*, vol. 5, Nature Publishing Group, London, 2003, pp. 757–766.
- [26] D.J. Levitin, U. Bellugi, Musical abilities in individuals with Williams syndrome, *Music Percept.* 15 (1998) 357–389.
- [27] D.J. Levitin, V. Menon, J.E. Schmitt, S. Eliez, C.D. White, G.H. Glover, J. Kadis, J.R. Korenberg, U. Bellugi, A.L. Reiss, Neural correlates of auditory perception in Williams Syndrome: an fMRI study, *NeuroImage* 18 (2003) 74–82.
- [28] D.J. Levitin, K. Cole, A. Lincoln, U. Bellugi, Aversion, awareness and attraction: understanding hyperacusis in Williams Syndrome, *J. Child Psychol. Psychiat.* (in press).
- [29] C. Miani, P. Passon, A.M. Bracale, A. Barotti, N. Panzolfi, Treatment of hyperacusis in Williams syndrome with bilateral conductive hearing loss, *Eur. Arch. Otorhinolaryngol.* 258 (2001) 341–344.
- [30] D.L. Mills, Electrophysiological markers of abnormal brain function in Williams Syndrome. *Cognitive Neuroscience Society Meeting*, Suppl. *J. Cogn. Neurosci.* 10 (1998) (Abstract).
- [31] P. Morosan, J. Rademacher, A. Schleicher, K. Amunts, T. Schormann, K. Zilles, Human primary auditory cortex: cytoarchitectonic subdivisions and mapping into a spatial reference system, *NeuroImage* 13 (2001) 684–701.
- [32] A. Nigam, P.R. Samuel, Hyperacusis and Williams syndrome, *J. Laryngol. Otol.* 108 (1994) 494–496.
- [33] W.Y. Ong, L.J. Garey, Neuronal architecture of the human temporal cortex, *Anat. Embryol.* 181 (4) (1990) 351–364.
- [34] T. Paus, D.W. Perry, R.J. Zatorre, K.J. Worsley, A.C. Evans, Modulation of cerebral blood flow in the human auditory cortex during speech: role of motor-to-sensory discharges, *Eur. J. Neurosci.* 8 (1996) 2236–2246.
- [35] L.A. Perez-Jurado, Williams–Beuren syndrome: a model of recurrent genomic mutation, *Horm. Res.* 59 (Suppl. 1) (2003) 106–113.
- [36] L.A. Perez-Jurado, Y.K. Wang, R. Peoples, A. Coloma, J.F. Cruces, U.A. Franck, Duplicated gene in the breakpoint regions of the 7q11.23 Williams–Bourne syndrome encodes the initiator binding protein TFII-I and BAP-135, a phosphorylation target of BTK, *Hum. Mol. Genet.* (1998) 325–334.
- [37] J. Rademacher, V.S. Caviness, H. Steinmetz, A.M. Galaburda, Topographical variation of the human primary cortices and its relevance to brain mapping and neuroimaging studies, *Cereb. Cortex* 3 (1993) 313–329.
- [38] J. Rademacher, P. Morosan, T. Schormann, A. Schleicher, C. Werner, H.J. Freund, K. Sills, Probabilistic mapping and volume measurement of human primary auditory cortex, *NeuroImage* 13 (2001) 669–683.
- [39] M.E. Raichle, What words are telling us about the brain, *Cold Spring Harbor Symp. Quant. Biol.* 61 (1996) 9–14.
- [40] A. Reiss, S. Eliez, J.E. Schmitt, E. Strous, Z. Lai, W. Jones, U. Bellugi, Neuroanatomy of Williams syndrome: a high-resolution MRI study, in: U. Bellugi, M. St. George (Eds.), *Special Issue: Linking Cognitive Neuroscience and Molecular Genetics: New Perspectives from Williams Syndrome*, *J. Cogn. Neurosci.*, MIT Press, Cambridge, MA, 2000, pp. 65–73.
- [41] K.S. Rockland, D.N. Pandya, Cortical connections of the occipital lobe in the rhesus monkey: Interconnections between areas 17, 18, 19 and the superior temporal gyrus, *Brain Res.* 212 (1981) 249–270.
- [42] P. Satz, E. Strauss, J. Wada, D.L. Orsini, Some correlates of intra- and interhemispheric speech organization after left focal brain injury, *Neuropsychology* 26 (2) (1988) 345–350.
- [43] P. Schneider, M. Scherg, H.G. Dosch, H.J. Specht, A. Gutschalk, A. Rupp, Morphology of Heschl’s gyrus reflects enhanced activation in the auditory cortex of musicians, *Nat. Neurosci.* 5 (2002) 688–694.
- [44] L.D. Selemon, G. Rajkowska, P.S. Goldman-Rakic, Abnormally high neuronal density in the schizophrenic cortex. A morphometric analysis of prefrontal area 9 and occipital area 17, *Am. J. Psychiatry* 52 (1995) 805–818.
- [45] J. Sergent, S. Ohta, B. MacDonald, Functional neuroanatomy of face and object processing. A positron emission tomography study, *Brain* 115 (1992) 15–36.
- [46] L. Shen, X. Hu, E. Jacoub, K. Ugurbil, Neural correlates of visual form and visual spatial processing, *Hum. Brain Mapp.* 8 (1999) 60–71.
- [47] R.B.H. Tootell, A.M. Dale, M.I. Sereno, R. Malach, New images from human visual cortex, *Trends Neurosci.* 19 (1996) 481–489.
- [48] L.G. Ungerleider, M. Mishkin, Two cortical visual systems, in: D.J. Ingle, M.A. Goodale (Eds.), *Analysis of Visual Behavior*, MIT Press, Cambridge, MA, 1982.
- [49] C. von Economo, G.N. Koskinas, *Die cytoarchitektonik der hirnrinde des erwachsenen menschen*, Springer, Berlin, 1925.
- [50] Y.K. Wang, C.H. Samos, R. Peoples, L.A. Perez-Jurado, R. Nusse, U. Francke, A novel human homologue of the *Drosophila* frizzled wnt receptor gene binds wingless protein and is in the Williams syndrome deletion at 7q11.23, *Hum. Mol. Genet.* (1997) 465–472.
- [51] R.W. Williams, P. Rakic, Three-dimensional counting: an accurate and direct method to estimate numbers of cells in sectioned material, *J. Comp. Neurol.* 278 (1988) 372–388.
- [52] P.I. Yakovlev, Whole-brain sections, in: C.G. Tedeschi (Ed.), *Neuropathology: Methods, Diagnosis*, Little, Brown, Boston, 1970.
- [53] K. Zilles, G. Schlaug, M. Matelli, G. Luppino, A. Schleicher, M. Qu, A. Dabringhaus, R. Seitz, P.E. Roland, Mapping of human and macaque sensorimotor areas by integrating architectonic, transmitter receptor, MRI and PET data, *J. Anat.* 187 (1995) 515–537.